

# The Wide Swath Ocean Altimeter: Algorithm and Technology Developments for Improved Ocean Topography Measurements

Brian D. Pollard, Ernesto Rodriguez, Amirit Kitiyakara, Torry Akins  
Jet Propulsion Laboratory  
California Institute of Technology  
4800 Oak Grove Drive  
Pasadena, CA 91109

**Abstract**—The Wide Swath Ocean Altimeter (WSOA) is a recently proposed interferometric instrument that would provide nearly complete global ocean topography measurements from a single platform. Several new algorithm and technology developments improve the expected WSOA performance, and facilitate the feasibility of including WSOA on a next generation altimeter mission. Those developments are discussed in this paper.

## I. INTRODUCTION

The TOPEX/Poseidon (T/P) mission demonstrated clearly the possibility of using nadir altimetry to obtain centimetric accuracy in measuring ocean topography. However, the temporal and spatial sampling characteristics of nadir-looking altimeters like T/P are such that the full spatial spectrum of oceanic variability cannot be observed: the 10 day repeat period required to avoid tidal aliasing means that T/P has equatorial gaps of approximately 300 km, much larger than a typical mesoscale ocean feature.

In [1], Rodriguez et al. propose a new measurement concept, a Wide Swath Ocean Altimeter (WSOA), that allows nearly complete global coverage of the ocean spatial spectrum while maintaining the 10 day repeat orbit of T/P, all from a single platform. The WSOA mission concept adds an across-track interferometer to a standard, T/P-like altimeter suite to obtain a swath of 200km. This interferometer, similar in concept to the recent Shuttle Radar Topography Mission (SRTM), uses a novel self calibration technique to eliminate the stringent requirements on baseline metrology, and to allow for centimetric height accuracy. This technique is described in detail in [1].

In addition to the self calibration technique, several other technology challenges must be met in order to equal the height accuracy of nadir-looking instruments: an interferometric baseline and antenna support structures must be within rigid stability criteria, and new interferometric

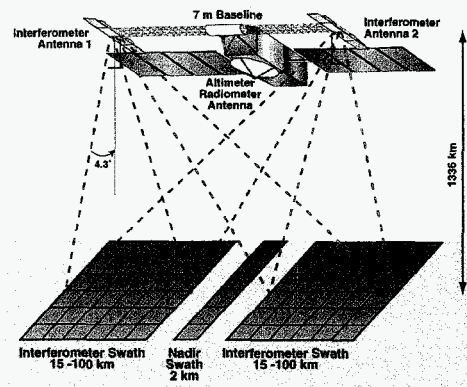


Figure 1. The WSOA mission concept.

height algorithms must be developed. We detail many of those developments in this short paper.

Finally, the desire to include the WSOA interferometer as a part of a next generation altimeter mission places considerable requirements on the instrument mass, power, and data rate. In this paper we discuss two of our solutions to those problems: a next generation, low mass, monolithic microwave integrated circuit (MMIC) three frequency radiometer; and a low power onboard data processor for data rate reduction.

The plan of this paper is as follows. The next section briefly reviews the WSOA mission concept. Section III discusses recent algorithm developments for improving the interferometric height accuracy of the WSOA interferometer. Section IV then introduces prototypes of three main WSOA technology drivers: the lightweight, ultra-stable deployable antenna structure; the next generation three frequency microwave radiometer; and a low power, high-throughput onboard data processor. We conclude with a brief summary in Section V.

Table 1: Key WSOA interferometer parameters.

Parameter	Unit	Value
Center Frequency	GHz	13.28
Bandwidth	MHz	20
Pulse Length	us	90
Pulse Repetition Frequency	Hz	1036
Peak Transmit Power	W	120
Antenna Width	m	0.3
Antenna Length	m	2.5
Antenna Boresight	deg	3.3
Baseline Length	m	6.4

## II. MISSION CONCEPT

Figure 1 presents the WSOA mission concept. A standard, T/P-like altimeter and radiometer suite is supplemented by a Ku-band across track radar interferometer. The interferometric baseline is created by a deployable 6 to 7 meter boom, with deployable Ku-band reflectarray antennas at each end. The interferometer is a dual-swath system, alternatively illuminating the left and right swaths. Each swath is 85 km in extent, starting at 15 km from the nadir track and extending to 100 km from the nadir track, creating an overall swath of 200 km. The pixel resolution of the interferometric system is 14 km by 14 km. The key radar parameters are given in Table 1.

As discussed in [1], in a T/P like orbit (1336 km, 66 degree inclination, 10 day repeat) the WSOA mission obtains nearly complete global coverage in a 10 day cycle. Figure 2 shows an example coverage map, where the color table represents the number of times a given 0.1 degree cell is sampled in a 10 day cycle. Such coverage would allow for study of mesoscale eddies, which typically have spatial scales of 100 km, and temporal scales of 30 days.

## III. RECENT ALGORITHM DEVELOPMENTS

The height estimation algorithms for WSOA were originally presented in [1]. In this section, we discuss some minor changes to those algorithms. Those changes, while minor algorithmically, improve substantially the expected WSOA height precision.

The WSOA instrument has heritage from nadir altimeters, such as T/P, and interferometric Synthetic Aperture Radar (SAR) systems, such as the SRTM. However, in at least three ways, WSOA presents unique challenges for height

estimation algorithms: the height precision goal is on the order of a few centimeters, two orders of magnitude finer than SRTM; the downlink data rate goal is on the order of 10 kbps, three to four orders of magnitude below that of an interferometric SAR; and, finally, the WSOA instrument is a real aperture system rather than a SAR.

We can first address the downlink data rate. The goal for WSOA is to reduce this rate to something comparable to a typical nadir altimeter, or to at least 10 to 20 kbps. Such a goal requires that a significant fraction of the interferometric processing occur onboard the spacecraft. However, in order to meet the centimetric height requirements, the processing must avoid approximations that may limit performance.

For a real aperture interferometric radar, height errors occur due to decorrelation between the two interferometric channels. The sources of decorrelation are:

- *Thermal noise*
- *Geometric decorrelation*: at boresight, the speckle of the two returns is slightly different,
- *Angular decorrelation*: iso-phases and iso-range lines are not aligned, leading to some decorrelation across each pixel
- *Pixel misregistration*: any misalignment of pixels also leads to decorrelation.

Figure 3 shows an example of the various decorrelation sources without any onboard data processing.

The onboard processing algorithm for the WSOA has been designed so that both misregistration and geometric decorrelation effects are minimized. Due to the fact that the two interferometric receivers are separated by the interferometric baseline, signals from the same point on the ground will arrive at different times at the receivers. It is possible to add a

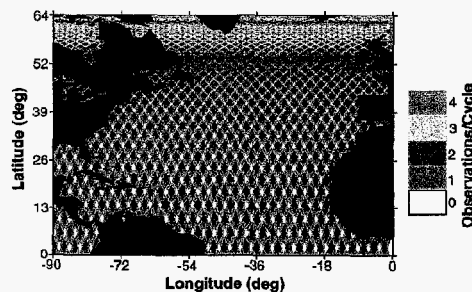


Figure 2. Example WSOA coverage. The color table represents the number of observations from WSOA in any given 0.1 degree cell in a 10 day cycle.

single delay between the channels so that the signals are coregistered for a given incidence angle. However, residual misregistration will still occur away from the selected direction. To achieve co-registration for the entire swath, we combine range compression and co-registration by using chirp-scaling [2, 3] to sample both image channels so that co-registration occurs at the surface. Unlike standard interferometric SAR processing, this step is possible at the range compression stage due to the lack of subsequent azimuth processing. Accurate co-registration can easily be performed for the ocean due to the lack of large surface slopes and the well known mean sea surface height.

The source of geometric decorrelation is the fact that the interferometric phase is not constant for all the scatterers within a given resolution cell. This variation in the interferometric phase causes the total interferometric contribution from that cell to add slightly incoherently, thus reducing the signal correlation.

Gatelli et al. [4] address this problem as follows: suppose that one is dealing with monochromatic signals, and chooses the wavelengths of the two channels to be such that the projected wave vectors on the ground are identical for both channels. In this case, the interferometric phase is constant for all scatterers in the resolution cell, and the returns add coherently.

When dealing with a finite bandwidth signal, things are a bit more complicated, but Gatelli et al. provide a solution: take the signal from both channels and shift the spectra in such a way that the appropriate wavelengths are multiplied together so that the phase variation over the resolution cell is canceled. This spectral shift means that noise is now brought into the processing bandwidth. In order to remove this additional noise, Gatelli et al. propose to use a low-pass filter so that only the parts of the spectra which overlap contribute to the interferometric return. The penalty for this low-pass filter is a loss in resolution, but this loss is usually small and acceptable. Unlike the case of SAR interferometry, it can be shown that for real aperture interferometers that the wavenumber shift removes geometric decorrelation effects, but does not remove angular decorrelation effects.

The wavenumber shift can be integrated with the last step of range compression and chirp scaling, so that only an additional FIR filter, which is computationally inexpensive, must be

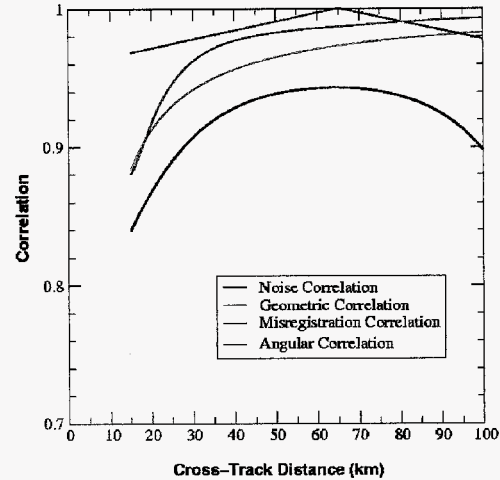


Figure 3. Example decorrelation values before onboard processing.

added to the processor. At the end of onboard processing, an azimuth averaged interferogram is produced which is down linked, so that the final height estimation can be performed on the ground. Since the interferogram can be averaged along-track, a significant gain is made in the total data which must be transmitted to the ground, so that the final data rate is of the same order of magnitude as for conventional altimetry.

All the processing steps described above are well understood mathematically, so that it is possible to get a full error budget for the random error component of the height error. In Table 2, we present the height error for two possible WSOA configurations. The first one, which has been designed to fit within the limitations of the attitude control system and power allocation of the Proteus bus (which will be used in the forthcoming Jason mission), uses a 6.4 m interferometric mast: it is designed to be a demonstration instrument to prove the concept of wide-swath ocean mapping. The second configuration, which uses a 10 m interferometric mast, is representative of the mapping capabilities of an operational WSOA mission. As can be seen from this table, even for off-nadir mapping, it is possible to achieve centimetric level precision while covering 200 km swaths.

The height accuracies quoted here do not include systematic errors, such as those due to spacecraft roll. It has been shown in [1] that these errors can be removed to centimetric level accuracy by using the cross-over regions to provide calibration.

Table 2. Estimated random height error (precision) after onboard processing.

Cell Center (km)	6.4 m Mast Height Error (cm)	10 m Mast Height Error (cm)
22.1	4.1	2.3
36.4	3.3	1.8
50.7	2.9	1.5
65.0	2.8	1.5
79.2	3.1	1.5
93.5	3.9	1.8

These height accuracies are also the single visit height accuracies. However, during a 10-day repeat cycle, the same point in the ocean will typically be mapped two to four times by ascending and descending passes, due to the wide swath characteristics of the instrument (see Fig. 2). These measurements may be combined by averaging, optimal interpolation, or assimilation to reduce the effective height error by a factor of 40% to 100%.

#### IV. TECHNOLOGY PROTOTYPES

In addition to the algorithms described above and in [1], the accuracy and accommodation requirements of WSOA require several further technology developments. In this section, we describe three such technologies, developed and tested over the last three years with Instrument Incubator Program (IIP) funding. These include: a deployable reflectarray antenna structure; a low mass, low power three frequency radiometer; and an onboard data processor that substantially reduces the downlink data rate.

##### A. Deployable Reflectarray Antenna Structure

The dominant source of systematic error (accuracy) in the WSOA interferometer is the antenna position knowledge and phase center stability. As an example, in order to obtain centimetric accuracy, the relative phase center between the two antennas must vary by less than 0.1 degrees. Thus, the structural stability of the antennas is of prime importance.

As part of our IIP effort, we have developed a novel deployable reflectarray concept. The deployable support structure (DSS) of this antenna, critical in maintaining phase center stability, has been designed and developed by AEC-Able Corporation, with outstanding results.

In Figure 4, the deployment sequence for the DSS is illustrated. The top panel shows the

stowed antenna, the second panel shows the antenna partially deployed, and the bottom panel shows the antenna fully deployed. The size of the antenna aperture after full deployment is 0.3 m by 2.5 m. The mass of the structure, without panels, is 3.6 kg; for the flight unit, that mass will be reduced to below 2.4 kg.

The testing performed on the antenna prototype structure included repeatability testing (better than 0.15 mm in all dimensions) and correlation of components with thermal models. All results were extremely favorable, suggesting that the developed antenna design is certainly capable of maintaining the required phase stability.

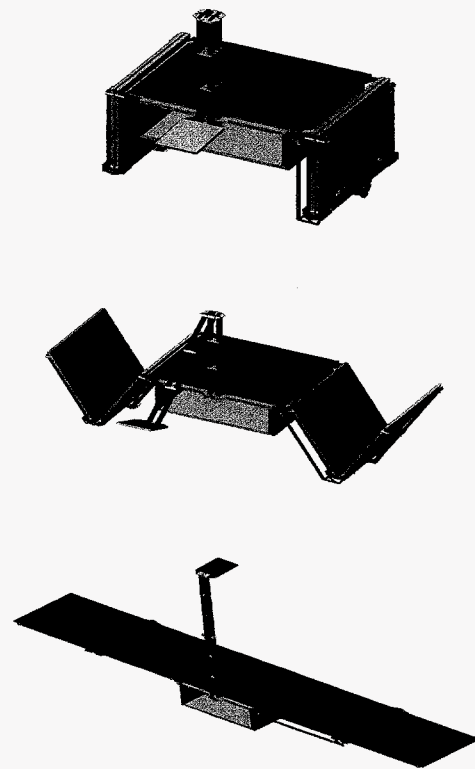


Figure 4. The WSOA interferometric antenna deployment sequence.

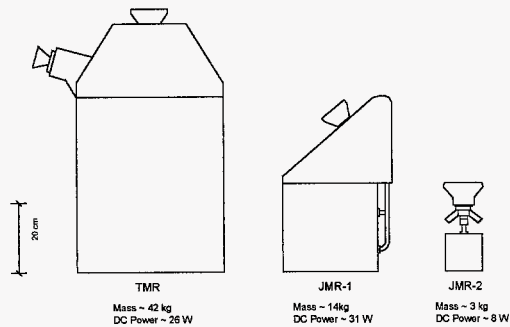


Figure 5. Size, mass, and power comparisons of the next generation radiometer (JMR-2) compared to the units aboard TOPEX (TMR) and Jason-1 (JMR-1).

### B. Next Generation Three Frequency Radiometer

1) *Microwave Radiometer & Calibration Noise Source:* The three frequency microwave radiometer provides altimeter range correction for path delay due to tropospheric water vapor. We have sought to enable a new generation radiometer system for the WSOA mission, with improved performance; significantly reduced, size, mass, and power; and greatly simplified electrical interfaces.

The elimination of bulky, narrowband ferrite Dicke switches in favor of broadband planar monolithic microwave integrated circuit (MMIC) PIN diode switches has enabled the integration of the three radiometer channels into one module with a single, broadband, ridged waveguide input. This compact, planar front-end architecture and the elimination of the multiple waveguide feeds with their associated thermal gradients has also served to reduce the sources of potential radiometer calibration error. Figure 5 shows a comparison of the WSOA/JMR-2 (Jason Microwave Radiometer-2) design to the T/P (TMR) and Jason-1 (JMR) microwave radiometers, while Figure 6 shows a photo of the brassboard radiometer.

In addition, as part of this effort, we have developed a brassboard calibration noise source module. This noise source, with integrated ridged waveguide coupler, mounts between the feedhorn and radiometer input and injects a noise signal for radiometer gain calibration.

2) *Multi-Octave Feedhorn:* We have also developed, with the Microwave Engineering Corporation (MEC), a novel five frequency feedhorn that will enable a single antenna system to be shared between the altimeter and the

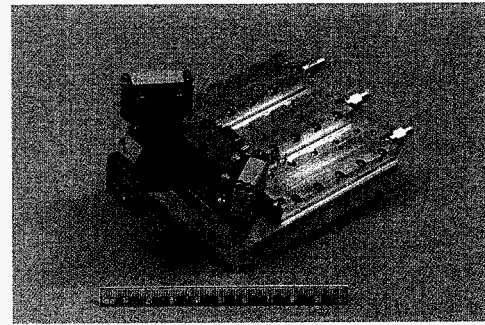


Figure 6. Three frequency radiometer brassboard.

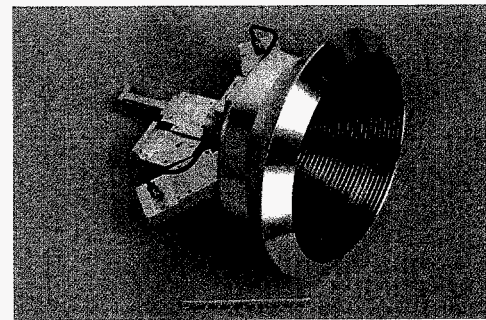


Figure 7. The multi-octave feedhorn brassboard.

radiometer. This elimination of the dedicated radiometer feedhorn and reflector simplifies the spacecraft configuration and increases the options in accommodating the proposed WSOA instrument on a small spacecraft. The IIP funding enabled the fabrication and testing of a brassboard version of this feedhorn design, which is a result of JPL funded MEC studies dating back to 1995. This feedhorn supports both the C and Ku band altimeters as well as the 18.7, 21.0, 34.0 GHz radiometer channels. Figure 7 shows a photo of the multi-octave feedhorn brassboard.

### D. Onboard Processor

While the expected raw data rate of the WSOA interferometer is quite high (see Table 3 below), much of the required processing to this data is straightforward, and thus a candidate for onboard processing. The onboard implementation of the range compression and interferogram formation, along with substantial amounts of along- and cross-track averaging, allow for a substantial reduction in the downlink data rate (as low as 20 kbps).

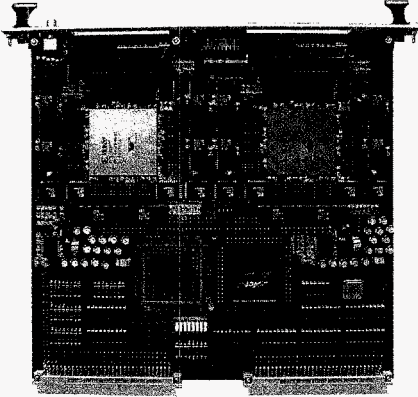


Figure 8. The FPGA-based VME prototype onboard processor card.

As a part of our technology demonstration process, we have developed a prototype onboard processor around the Xilinx Virtex Field Programmable Gate Arrays (FPGA). Each device contains 1 million SRAM based programmable gates. The prototype board is shown in Figure 8. Per our design, all of the components, including the FPGAs, have a space qualified equivalent part. The density and speed of the Xilinx FPGAs allow the entire onboard processor to be placed on a single VME card, while the reconfigurability of the device allows for the algorithm to change during the development and after launch.

The basic algorithm is quite straightforward: the processor range compresses the two interferometric channels, forms the complex interferogram, and averages to reduce the data rate. The key parameters for the onboard processor are given in Table 3.

An example of this result is shown in Figure 9. In this example, each data channel captures a 90 $\mu$ s chirp, performs the pulse compression, and calculates the complex conjugate result. Each processor can perform these operations in less than 1ms, thus allowing for a single side PRF of greater than 1kHz.

Table 3. Onboard processor parameters.

Parameter	Unit	Value
VME Card Mass	kg	3
DC Power Usage	W	15
Processor Clock Rate	MHz	30
Input Data Rate	Mbps	262
Output Data Rate	kbps	20
Total Computation Rate	GOPS	21

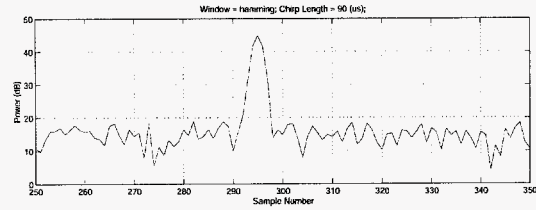


Figure 9. Example compressed pulse, including expected thermal noise.

#### IV. SUMMARY

In this paper, we have introduced several of the algorithm and technology developments for a WSOA mission. A careful review of the onboard algorithms has allowed us to improve the expected WSOA height precision from the results reported in [1]. Successful prototype developments of a deployable antenna structure, next generation radiometer, and onboard processor have also been described.

#### ACKNOWLEDGEMENT

This work was performed by the Jet Propulsion Laboratory, California Institute of Technology, under contract with the National Aeronautics and Space Administration (NASA). The authors wish to acknowledge Steve White, Jason Schmidt, David Messner, Gary Heinemann, and the other members of the AEC-Able antenna prototyping team for their excellent work on the deployable antenna structure.

#### REFERENCES

- [1] E. Rodriguez, B.D. Pollard, and J.M. Martin, "Wide swath ocean altimetry using radar interferometry," *IEEE Trans. Geoscience and Remote Sensing*, in press.
- [2] L. Rabiner, R. Schaffer, and C. Rader, "The chirp-z transform and its applications," *Bell Syst. Tech. J.*, vol 48, 1249-1292, 1969.
- [3] R.K. Raney, H. Runge, R. Bamler, I. Cumming, and F. Wong, "Precision SAR processing using chirp scaling," *IEEE Trans. Geoscience and Remote Sensing*, vol 32, pp 786-799, 1994.
- [4] F. Gatelli, A. Monte-Guarnieri, F. Parizzi, P. Pasquali, C. Parti, and F. Rocca, "The wavenumber shift in SAR interferometry," *IEEE Trans. Geoscience and Remote Sensing*, vol. 32, no. 4, 855-865, 1994.